APPENDIX

Temperature-dependent body size effects determine population responses to climate warming

Max Lindmark†[1], Magnus Huss[1], Jan Ohlberger[2], Anna Gårdmark[1]

[1]Swedish University of Agricultural Sciences, Department of Aquatic Resources, Institute of Coastal Research, Skolgatan 6, SE-742 42 Öregrund, Sweden

[2]School of Aquatic and Fishery Sciences, University of Washington, Seattle, WA 98195, USA

† Author to whom correspondence should be addressed. Current address:

Max Lindmark, Department of Aquatic Resources, Institute of Coastal Research, Swedish University of Agricultural Sciences, Skolgatan 6, Öregrund 742 42, Sweden, Tel.: +46(0)104784137, email: max.lindmark@slu.se

PARAMETERIZATION OF THE STAGE-STRUCTURED BIOMASS MODEL ACCOUNTING FOR SIZE- AND TEMPERATURE-DEPENDENCE OF VITAL RATES

Body-size

We based our parameterization of temperature-dependence in the stage-structured biomass model on the fish species roach (*Rutilus rutilus*), but the modelling framework and studied mechanisms apply to other organisms exhibiting size- and food-dependent development, i.e. most animal organisms (de Roos and Persson, 2013). As we model life stages with different body sizes rather than continuous size-distributions, we estimated representative weights of juveniles, m_J, from the equation: $m_J = m_{max} - m_{min} / \ln(m_{\max} - m_{min})$, where m_{min} is the weight of consumers at the onset of active feeding and m_{max} is the weight at maturation (van Leeuwen *et al.*, 2008). This resulted in a juvenile size of 3.9 g. m_{min} and m_{max} were acquired by converting published estimates of initial consumer length (s_h) and length at maturation (s_m) to weight using the length-weight relationship $\lambda_1 m^{\lambda_2}$ (Table S1). We assumed s_h, the length at the onset of active feeding, to be approximately twice the length at hatching (Byström and García-Berthou, 1999). As adults in the model do not grow in size after reaching maturation, their average weight, m_A, was given by m_{max} (32.4 g). The initial to adult body size ratio in the maturation function (z) was given by the ratio $m_{min}/m_{\max}$, providing a value of 0.00025 (Table

S1). At equal maturation and reproduction rates in the population, the adult to juvenile stage biomass ratio is not 1:1 but equals $-\ln(z)$, where z is the ratio of juvenile to adult individual mass. This means that for $z < e^{-1}$, the juvenile to adult ratio is larger than one (de Roos and Persson, 2013)

Mass- and temperature-dependence of vital rates

The temperature-dependence of maximum intake rate, $I_{max,i}(T, m)$, was acquired by statistically estimating the parameter E_I from experiments using roach weighing between 1.2 to 300 g fed ad libitum at temperatures between 5°C and 20°C (data provided in Hölker (2000); see also Hölker and Haertel (2004)). Our estimate of $E_I = 1.21\ eV$ (Table 2) was substantially higher than what is predicted by the MTE (0.6-0.7 eV) (Brown *et al.*, 2004), but within the wide range of empirical estimates presented in Englund *et al.* (2011). The effect of the value of the parameter E_I for population regulation was tested separately (see '*Varying activation energy of the functional response relative to metabolic rate'*, this document*)*. Based on the same data (Hölker, 2000), the temperature- and mass interaction parameter, c_I, was estimated to be -0.012, suggesting that the mass exponent of maximum intake in roach is reduced in warmer environments relative to the exponent of metabolism, which in roach does not change with temperature (Ohlberger *et al.*, 2012) (Note that in the modelling analysis we instead vary temperature-dependence on metabolic rate relative to functional response parameters – see '*Methods*' in main text). Hjelm and Persson (2001) estimated a mass-dependent attack rate ($a_i[T, m]$) of roach feeding on 1-mm zooplankton prey (*Daphnia sp.*) at 19°C. We defined the reference temperature as 19°C (292.15 K), which removed the need to re-estimate the normalization constant $B_0(T_0)$ (see equation in '*Introduction*', main text) estimated from empirical data. We could not find published studies estimating a temperature- and mass dependent attack rate of roach. However, as we analyzed the effect of differences in temperature-dependence between metabolic costs versus actual ingestion, rather than the parameters of the functional response, we assumed equal E_I for attack rate and maximum intake rate – but see Englund *et al.* (2011).

Metabolic rate parameters c_M and E_M (Table 1 and 2) were acquired from Ohlberger *et al.* (2012), in which the interaction between mass and temperature was explicitly estimated, after converting metabolic rate to unit g wet weight from J g^{-1} (Lumb *et al.*, 2007; Beier, 2016; Pothoven *et al.*, 2006).

We let background mortality scale with mass and temperature based on the theoretical prediction that it should scale similarly as the mass-specific metabolic rate and maximum population growth rate interspecifically (Brown *et al.*, 2004; Savage *et al.*, 2004). This prediction was tested in Savage *et al.* (2004) based on mortality rates for 175 marine fish stocks compiled by Pauly (1980). More specifically, Savage *et al.* (2004) found that it was in close agreement with both the prediction of a quarter-power scaling with mass and an activation energy (0.45 eV) similar to that for metabolic rate of fish (Gillooly *et al.*, 2001). This estimate is lower than our estimated activation energy for metabolic rate for roach (0.594 eV) (Ohlberger *et al.*, 2012), which could be due to the former being an interspecific average

whereas the latter is an intraspecific estimate. We used a value of 0.0015 for the mass scaling constant of mortality (Table 2), rescaled to 19°C by de Roos and Persson (2013) based on the mass- and temperature-dependent scaling presented in Gillooly *et al.* (2001)). We do not include temperature-dependence in the allometric exponent of mortality rate, as we want to focus specifically on the temperature-dependent size-scaling of metabolism relative to that of ingestion. Mortality also influences stage-specific performance, but it is less influential for population regulation than stage-specific resource availability and scaling of ingestion and metabolic rate (Persson and de Roos, 2013).

Lastly, assimilation efficiency (σ) is often assumed to be independent of mass and temperature (Peters, 1983). This may not always be the case, however, and a temperature-dependent assimilation efficiency may also influence the size-based competitiveness that shapes population regulation. To clearly contrast the effects of different scaling of food ingestion relative to metabolic rate, for which we have reliable data, we assumed size- and temperature independent assimilation efficiency.

Resource

We assumed that temperature affects the resource growth only through the maximum growth rate δ(T), and not the maximum resource biomass density, R_{max}. The maximum resource growth rate is thought to be mainly constrained by the temperature-dependence of metabolic rate, which the Arrhenius equation explains well at biologically relevant temperatures (Gillooly *et al.*, 2001; Savage *et al.*, 2004). We estimated the activation energy of resource turnover rate, E_δ, by fitting a non-linear least square regression using the R-function $nls()$ to the increasing part of the unimodal temperature-dependence used in Ohlberger *et al.* (2011a). From metabolic scaling principles it can be predicted that R_{max} ('carrying capacity') should decrease with temperature due the increased feeding needed to balance increased metabolic costs (given temperature-independent nutrient supply) (O'Connor *et al.*, 2011; Savage *et al.*, 2004; Uszko *et al.*, 2017). However, it is often influenced by additional abiotic factors (Gilbert *et al.*, 2014; Uszko *et al.*, 2017), and recent experimental studies suggest that carrying capacity can even be temperature-independent in algae across a large temperature range (Uszko *et al.*, 2017). As δ(T) and R_{max} only affect the total consumer biomass, but not the juvenile to adult biomass ratio nor the qualitative population regulation (Fig. S2) (Ohlberger *et al.*, 2011b), we assumed a temperature-independent maximum resource biomass density in line with previous studies (Vasseur and McCann, 2005; Ohlberger *et al.*, 2011a; see also Uszko *et al.*, 2017).

Table S1 Model variables and default parameter values.

Symbol	Value	Unit	Interpretation	Reference
Variables				
$\boldsymbol{R}$	–	$\mathbf{g/100m^3}$	Biomass density of shared resource	
$\boldsymbol{R_A}$	–	$\mathbf{g/100m^3}$	Biomass density of adult resource	
$\boldsymbol{J}$	–	$\mathbf{g/100m^3}$	Juvenile biomass density	
$\boldsymbol{A}$	–	$\mathbf{g/100m^3}$	Adult biomass density	
Temperature				
$\boldsymbol{T}$	$\boldsymbol{varied}$	**K**	Temperature	
$\boldsymbol{T_0}$	$\mathbf{292.15}$	**K**	Reference temperature	
Ontogeny				
$\boldsymbol{s_h}$	**12**	**mm**	Length at onset of active feeding	Byström and García-Berthou (1999)
$\boldsymbol{s_m}$	**140**	**mm**	Length at maturation (adult size)	Stoessel (2014)
$\boldsymbol{\lambda_1}$	$\mathbf{0.00794}$	$\mathbf{mm\ g^{-\lambda_2}}$	Constant in length-weight-relationship	Froese *et al.* (2014)
$\boldsymbol{\lambda_2}$	$\mathbf{3.15}$	–	Exponent in length-weight-relationship	Froese *et al.* (2014)
Mortality				
$\boldsymbol{\varphi_1}$	$\mathbf{0.0015}$	$\mathbf{g^{(1-\varphi_2)}\ day^{-1}}$	Allometric scalar of background mortality	Gillooly *et al.* (2001); de Roos and Persson (2013)
$\boldsymbol{\varphi_2}$	$\mathbf{0.75}$	–	Allometric exponent of background mortality	Gillooly *et al.* (2001)
$\boldsymbol{E_\mu}$	$\mathbf{0.45}$	**eV**	Activation energy of background mortality	Savage *et al.* (2004)
Resource				
$\boldsymbol{\delta}$	$\mathbf{0.1}$	$\mathbf{day^{-1}}$	Turnover rate of shared and adult resource	de Roos and Persson (2013)
$\boldsymbol{R_{max}}$	**1**	$\mathbf{g/100m^3}$	Maximum resource biomass density	van Leeuwen *et al.* (2008)
$\boldsymbol{x}$	**varied**	–	Factor scaling maximum biomass density of resource exclusive to adult relative to of the shared resource	
$\boldsymbol{E_\delta}$	$\mathbf{0.43}$	**eV**	Activation energy of resource turnover rate	Ohlberger *et al.* (2011a); Mitchell *et al.* (2004)
Consumption				
Â	**3**	$\mathbf{100m^3\ day^{-1}}$	Maximum zooplankton (1mm) attack rate	Hjelm and Persson (2001)
$\boldsymbol{m_o}$	**41**	**g**	Optimal forager size for 1mm zooplankton	Hjelm and Persson (2001)
$\boldsymbol{\alpha'}$	$\mathbf{0.75}$	–	Allometric exponent of attack rate at T_0	Hjelm and Persson (2001)
$\boldsymbol{\varepsilon_1}$	$\mathbf{0.25}$	$\mathbf{g^{(1-\varepsilon_2)}\ day^{-1}}$	Allometric scalar of maximum ingestion rate	Hölker (2000)
$\boldsymbol{\varepsilon_2{}'}$	$\mathbf{0.77}$	–	Allometric exponent of maximum ingestion rate at T_0	Hölker (2000)
$\boldsymbol{E_I}$	$\mathbf{1.21}$	**eV**	Activation energy of functional response parameters	Hölker (2000)
$\boldsymbol{c_I}$	**0**	$\mathbf{°C^{-1}}$	Temperature effect on mass-scaling exponent of ingestion	
$\boldsymbol{\sigma}$	$\mathbf{0.5}$	–	Assimilation efficiency	Ohlberger *et al.* (2011a); Karås and Thoresson (1992)
Metabolism				
$\boldsymbol{\rho_1}$	$\mathbf{0.0123}$	$\mathbf{g^{(1-\rho_2)}\ day^{-1}}$	Allometric scalar of metabolism	Ohlberger *et al.* (2012)
$\boldsymbol{\rho_2{}'}$	$\mathbf{0.77}$	–	Allometric exponent of metabolism at T_0	Ohlberger *et al.* (2012)
$\boldsymbol{E_M}$	$\mathbf{0.594}$	**eV**	Activation energy of metabolism	Ohlberger *et al.* (2012)
$\boldsymbol{c_M}$	**varied**	$\mathbf{°C^{-1}}$	Temperature effect on mass-scaling exponent of metabolism	Ohlberger *et al.* (2012)

BIOMASS-OVERCOMPENSATION IN RESPONSE TO INCREASED MORTALITY

We find initial increases in juvenile biomass in response to increased, stage-independent background mortality in the case of reproduction regulation (Fig. S1, left panel, dashed red line). A similar hump-shaped response is seen in the adult stage at high temperatures given that the population is regulated by a limited maturation (Fig. S1, right panel, dotted red line). These stage-specific biomass overcompensations (Fig. S1a, grey line) are consistent with size-structured theory, and can be understood from that mortality relaxes energetic bottlenecks in the population, which in turn is mediated by the interactive effect of size and temperature (c). Specifically, when temperature enhances the reproduction regulation in the consumer population ($c > 0$), there is biomass overcompensation (hump-shape) in the juvenile stage as a response to increased background mortality. This is due to the mortality-induced relaxation of the adult bottleneck which increases the reproductive output of adults (Fig. S1a, red dashed lines). By contrast, when $c = -0.02$, the population is maturation-regulated at 35 °C (Fig. S1) and the juvenile biomass at equilibrium declines over mortality (Fig. S1a, dotted lines). Adult biomass decreases with increased mortality in the case of reproduction-regulation (Fig. S1b, red dashed lines and grey lines), and show a hump-shaped mortality response otherwise

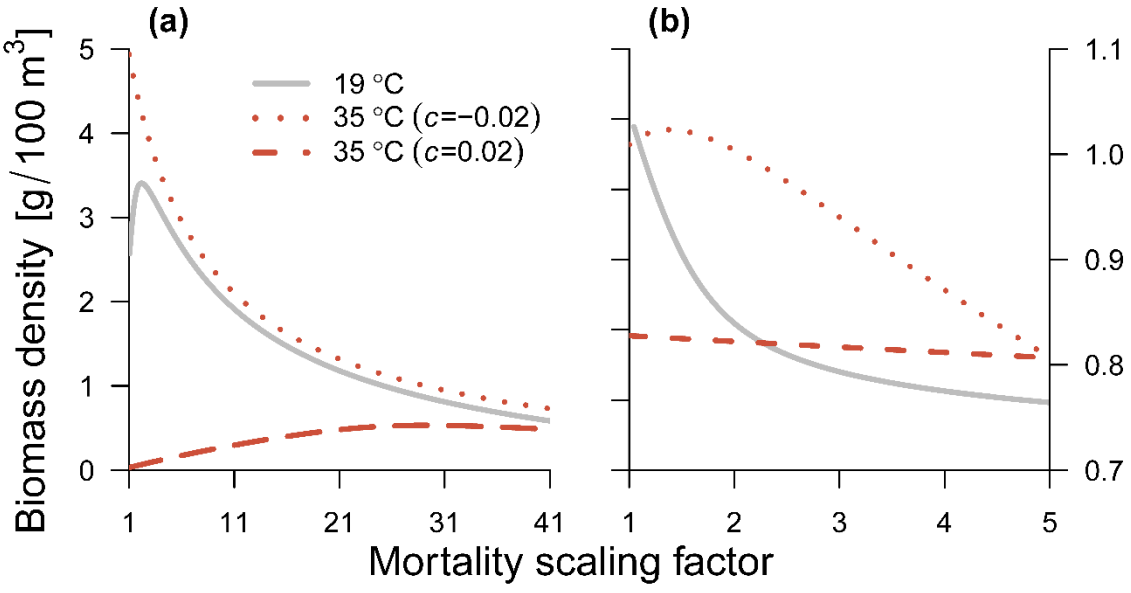

Figure S1 Equilibrium biomass density of juvenile (a) and adult (b) consumers as a function of background mortality scaling factor (1=default model), for reference ($T_0 = 19\,°C$) (solid grey line) and for a high ($T_0 = 35\,°C$) temperature, for negative ($c = -0.02$) (dotted red line) and positive ($c = 0.02$) (dashed red line) temperature effect on the exponent of metabolism. Right hand side y-axis correspond to negative c-effects (dotted red line).

GENERALIZING MODELLING RESULTS

Varying productivity of shared resource

In order to assess the influence of resource productivity on our conclusion about when and how population regulation and relative biomass densities of the consumer life stages is affected by temperature, we repeated our analysis (Fig. 3) using an increase in maximum resource biomass density ($R_{max} = 100$) (Fig. S2). The resource parameters govern the total biomass density of the consumer, but not the competitive balance between the life stages and thus not the ratio of juvenile to adult biomass density (Ohlberger *et al.*, 2011b). This is because if ingestion and mortality is equal for the two life stages, the biomass ratio between stages is constant (de Roos and Persson, 2013), and R_{max} does not affect the ratio between either of those two allometric functions. Thus, resource productivity does not influence the effect of temperature-dependence of allometric scaling, and the conclusions about the c-parameter and its potential effect on population regulation remain qualitatively equivalent to the default parameterization used in the main text.

Varying activation energy of the functional response relative to metabolic rate

We also analyzed the influence of the activation energy of functional response parameters relative to the activation energy of metabolic rate, E_I and E_M, respectively. The ratio between these parameters can influence consumer-resource stability (see main text). In addition, empirical analyses have revealed a large variation in the activation energy of functional response parameters (Englund *et al.*, 2011). We therefore repeated the analysis in Fig. 3 with a lower activation energy of functional response parameters relative to that of metabolic rate. This is an approximation of analyzing post-optimum temperature, as ingestion rate is a unimodal function over temperature while metabolic rate increases exponentially (Jobling, 1997). We choose a value of 0.4 for E_I, which stems from the lowest value in the confidence interval for attack rate in predatory fish, presented in Englund *et al.* (2011). The E_I: E_M ratio only slightly affects the temperature-response of consumer biomass density (Fig. S3). It does

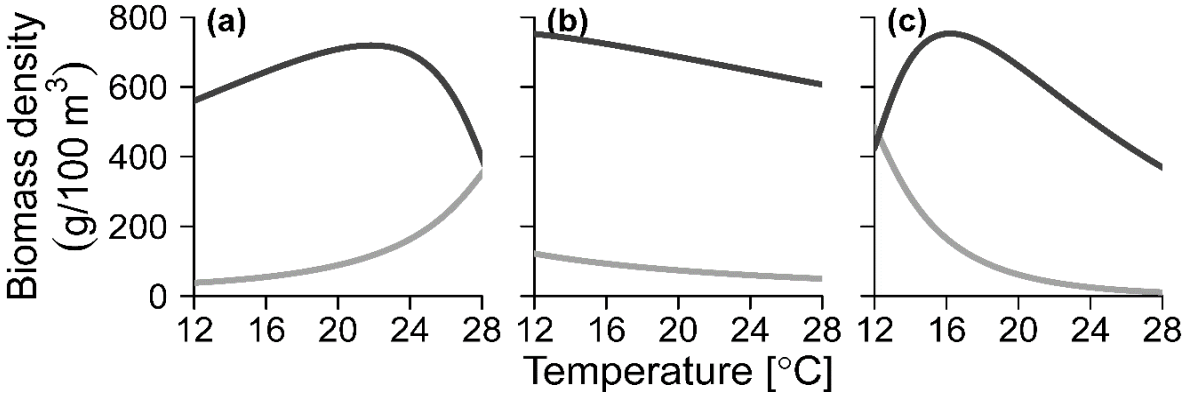

Figure S2 Equilibrium biomass density of juveniles (grey) and adults (dark grey) for negative (left), positive (right), and no temperature-dependence of metabolic allometry (centre) as a function of temperature. (a) shows model output assuming a negative temperature effect on the exponent of metabolism ($c = -0.02$), (b) corresponds to temperature independent allometry (c=0) and (c) shows the model output with positive temperature-dependence of the metabolic exponent ($c = 0.02$). Default model (see Fig. 3 in manuscript, but with with $R_{max} = 100$).

however limit the top down control of the resource, which increases over temperature due to the inefficient feeding by consumers (compare Fig. S3 and Fig. 3). As it does not affect the *size-based* performance it does not influence the mode of population regulation or how warming induces shifts in population regulation.

We also tested the influence of our assumption of equal activation energies of attack rate, a_i, and maximum ingestion, $I_{max,i}$, by analyzing the model with a temperature-independent attack rate (all else equal). This was done to analyze the effect of having two temperature-dependent rates in the functional response (Table 1). When activation energies for $I_{max,i}$ and a_i are identical, the ratio of juvenile to adult biomass-specific ingestion does not change over temperature for any given resource density (Fig. S4). By contrast, this ratio increases slightly with temperature when assuming a temperature independent attack rate. However, it does not influence our conclusions with respect to mode of population regulation and temperature-dependent size-scaling (Fig. S5).

Therefore, our general conclusion that interactive temperature- and size-scaling of vital rates alters population and stage-specific responses to rising temperatures, such that warming can induce shifts in population regulation, holds for a range of activation energies.

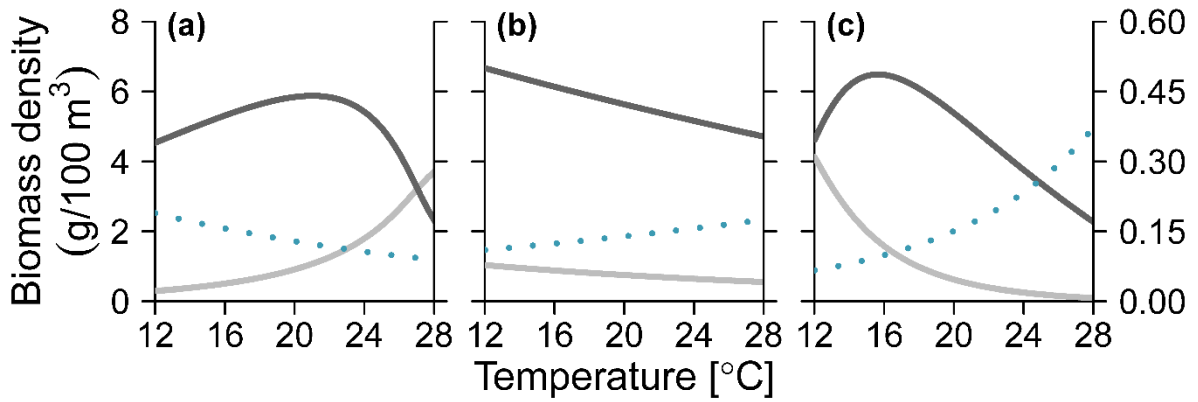

Figure S3 Equilibrium biomass density of juveniles (grey), adults (dark grey) and the resource (blue, dotted line) for negative (left), positive (right), and no temperature-dependence of metabolic allometry (centre) as a function of temperature. (a) shows model output assuming a negative temperature effect on the exponent of metabolism ($c = -0.02$), (b) corresponds to temperature independent allometry ($c = 0$) and (c) shows the model output with positive temperature-dependence of the metabolic exponent ($c = 0.02$). Default model (see Fig. 3 in manuscript, but with $E_I < E_M$ (0.4 and 0.594 respectively).

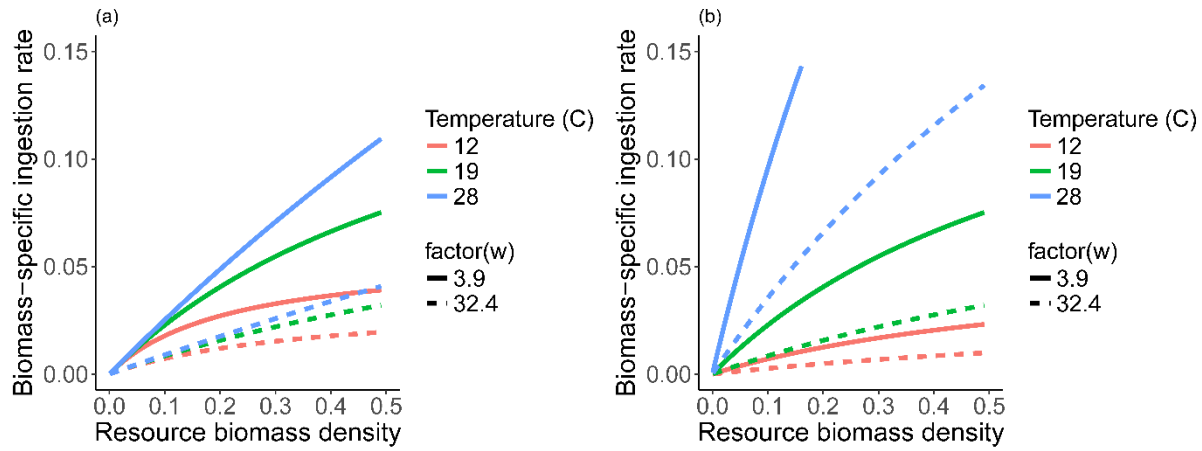

Figure S4 Functional response curves for juveniles (solid lines) and adults (dashed line) at 12 °*C (red),* 19 °*C (green) and* 28 °*C (blue). In panel (a), attack rate is assumed to be independent of temperature and in panel (b) it is assumed to have equal activation energy as maximum ingestion rate (default model) – see Table 1.*

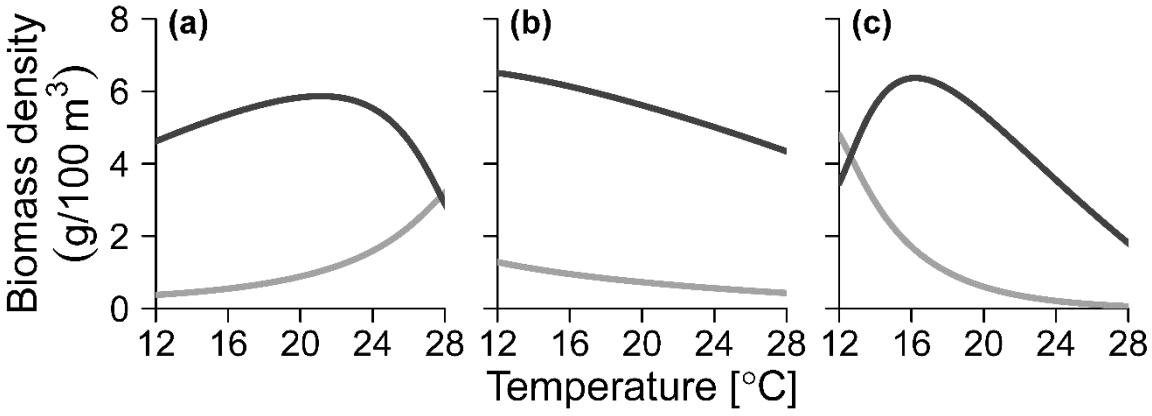

Figure S5 Equilibrium biomass density of juveniles (grey) and adults (dark grey) for negative (left), positive (right), and no temperature-dependence of metabolic allometry (centre) as a function of temperature. (a) shows model output assuming a negative temperature effect on the exponent of metabolism ($c = -0.02$), (b) corresponds to temperature independent allometry ($c = 0$) and (c) shows the model output with positive temperature-dependence of the metabolic exponent ($c = 0.02$). Default model (see Fig. 3 in manuscript, but with no temperature dependence of attack rate, $a_{J,A}$, only of maximum ingestion, $I_{max,i}$.

Effect of feeding proportion and productivity of resource exclusive to adults

In order to assess the interplay between intrinsic and extrinsic factors for population regulation and relative biomass densities of consumer life stages, we increased the feeding potential of adults by extending the food web to include a resource (R_A) exclusive to the otherwise less competitive adult stage. We performed a continuation of the equilibria at the reference temperature over the parameter determining the adult feeding proportion (p) (Fig. S6) in order to identify p-values resulting in stable fixed point dynamics, from which we then continued over temperature for different c-values. Equal productivities (with R_{max} representing 'productivity') resulted in a larger range of p-values giving rise to stable dynamics compared to when the resource productivity of the adult resource was lower than the shared resource (Fig. S6). The three p-values used in the main text for continuation of equilibrium over temperature were chosen such that both types of regulation were present at the reference temperature (Fig. 4; Fig. S6). By default, we assumed equal productivities of the shared and adult-exclusive resource in the main text, but here we also tested a lower productivity of the adult-exclusive resource (Fig. S.7).

We varied the productivity of R_A relative to R using the scaling factor x, such that $R_{max,A} = R_{max}x$, and $x < 1$ (Table S1). We assumed $x < 1$, as it represents a higher trophic level-resource that becomes available to consumers as they grow in size (see Table 1 for implementation). When the productivities of the shared and adult resources are equal, increased feeding proportions on the exclusive adult resource by adults rapidly makes them superior competitors, and the scaling of vital rates became relatively less influential in terms of mode of regulation (Fig. 4, main text). However, since the gains of adults from feeding on their exclusive resource depend on its productivity, we further generalize our results here by varying the productivity of R_A. With reduced productivity (in this case $x = 0.5$), the same qualitative pattern emerged, namely that when increasing temperatures benefit the stage constituting the bottleneck through size-specific effects, we observed shifts in population regulation (Fig. S7). When $x = 0.5$, the parameter space with symmetry (i.e. the transition between two modes of

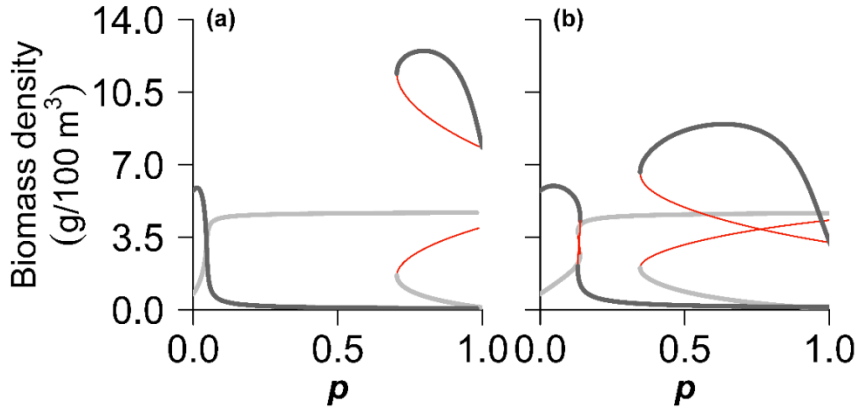

Figure S6 Continuation of equilibrium over p (proportion adults feed on their exclusive resource) at the reference temperature (all other parameters have default values) for (a) $x = 1$ and (b) $x = 0.5$. Thin red lines are unstable equilibria, juvenile and adult biomass correspond to grey and dark grey lines, respectively. With increased feeding proportion on exclusive resource, the population regulation shifts to a maturation-regulated system with competitively superior adults. Lower productivities of the exclusive resource lead to more bistable communities with respect to p.

regulation) induced by warming through the size- and temperature-dependent scaling of vital rates (i.e. intrinsic properties) occurred at slightly higher temperatures relative to when $x = 1$ (compare Fig. 4 main text with Fig. S7). In addition, when $x = 0.5$, continuation of the equilibrium curves over temperature results in a saddle-node bifurcation. Along the curves, regions of unstable saddle points emerge before stable equilibria with an altered mode of population regulation appear (Fig. S7). At sufficiently high p-values, alternative stable states emerged irrespective of c, although c determined when these appear in the temperature-p parameter space. As x was further reduced, the temperature range with bistability is increased (not shown).

Therefore, our conclusions hold when generalizing the food web to include extrinsic factors (in our case, broader feeding niche of one life stage), which together with the mass- and temperature-dependent rates affect the relative performance of consumer life stages. The effects of temperature-dependent size-scaling of vital rates become less influential for population regulation in the presence of strong extrinsic factors within the given temperature range. However, size-scaling still influences biomass responses to temperature, including presence of alternative stable states (Fig. S7). In essence, our models predict that warming can alter the mode of population regulation if temperature, through its effects on size-based individual performance, alters the competitive dominance between consumer life stages.

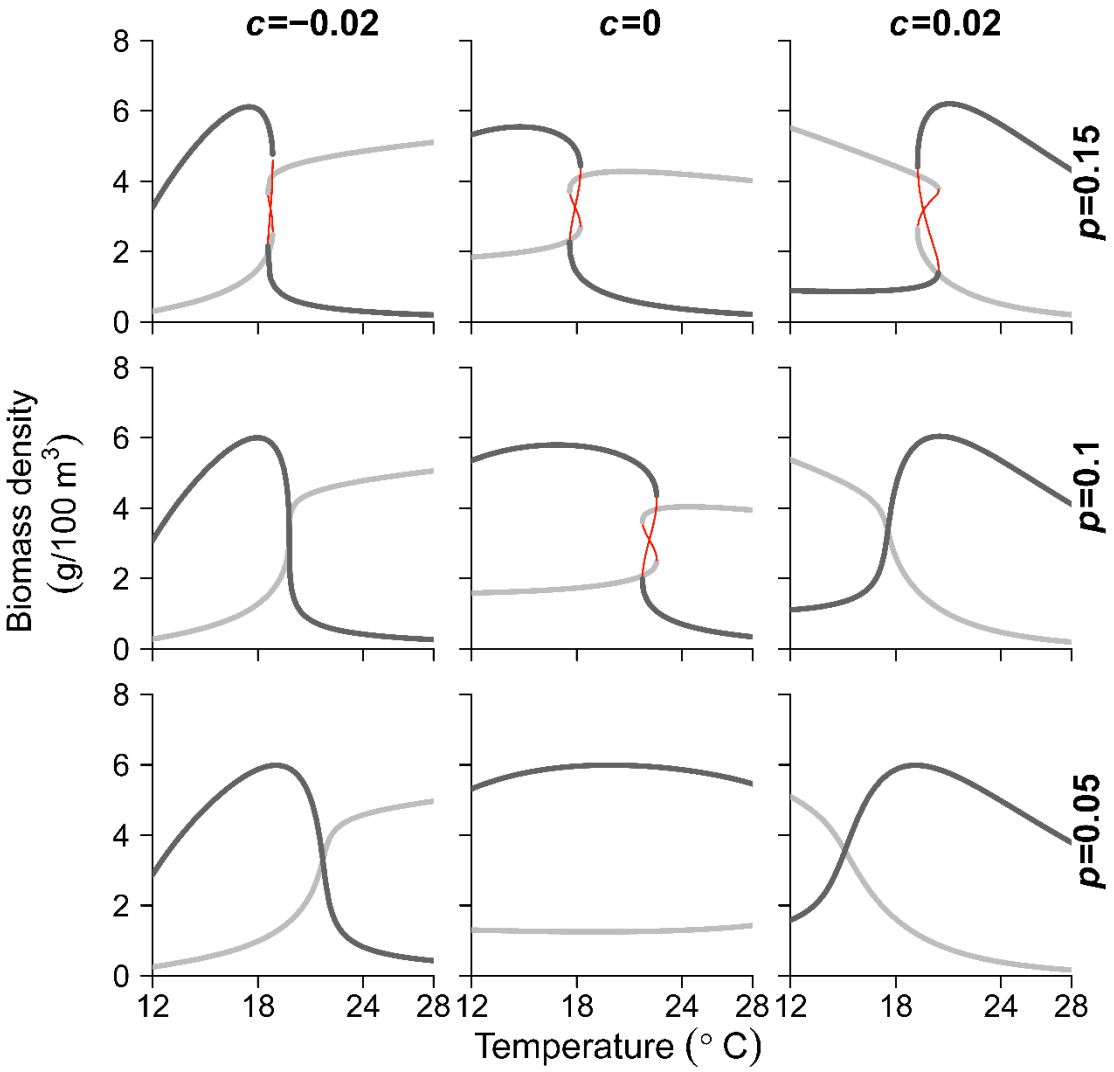

Figure S7 Equilibrium biomass densities over temperature given different feeding proportions of adults on their exclusive resource (p) and temperature dependence of metabolic rate exponent, c, when the productivity of the adult resource is half of the productivity of the shared resource ($x = 0.5$). Grey lines are juvenile biomass densities and black lines are adult biomass densities. Thin red lines correspond to unstable equilibria separating stable equilibria in the regions of bistability. p-values were chosen on the basis of maintaining similar equilibrium dynamics to when $p = 0$, for a clear contrast to scenarios where $p \neq 0$ (when $p > 0.7$ bistability occurs at the reference temperature, in contrast to the stable equilibrium observed when $p = 0$).

Logistic resource growth in default model

As we want to focus on the role of consumer energetics through temperature- and mass dependent scaling, we use semi-chemostat dynamics for the resource (see '*Dynamics of the stage-structured consumer-resource system*'). However, in order to assess the influence of our choice of resource dynamics, we performed the same analysis as in Fig. 3 but with logistic resource growth and the same set of parameters as for semi-chemostat growth ($K = R_{max}$ and $r = \delta$). When $c = -0.02$, the adult to juvenile biomass ratio decreases over temperature. This is predicted to occur in a population regulated by limited reproduction given negative c-effects (Fig. S8a). In addition, when $c = -0.02$ a supercritical Hopf bifurcation in which stable limit cycles appear at 26.4 °C (i.e. consumer-resource cycles) around the equilibrium point, which becomes unstable (Fig. S8). Note this bifurcation does not occur for other values of c (nor in the semi-chemostat model used in the main analysis).

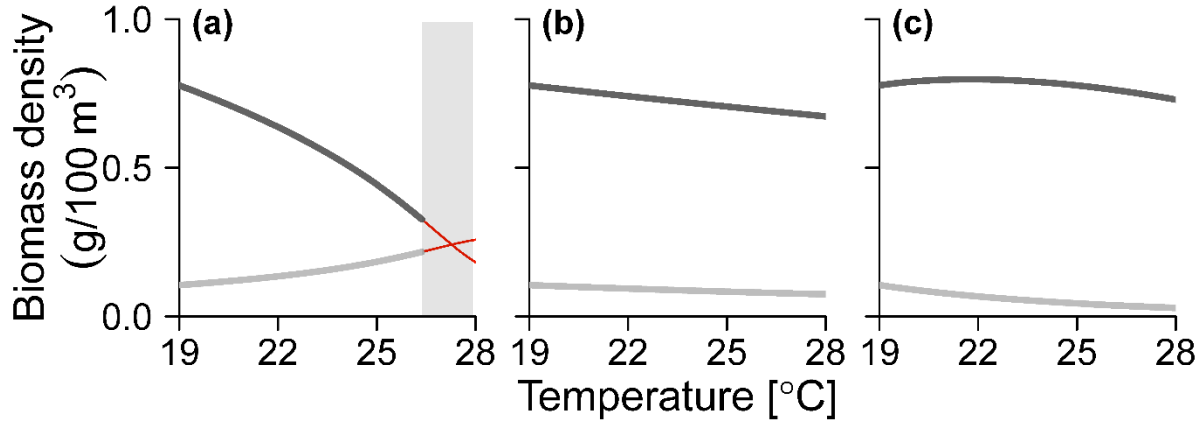

Figure S8 Equilibrium biomass density of juveniles (grey), adults (dark grey) and resource (blue dashed line) as a function of temperature, for negative (a), positive (c), and no temperature-dependence of allometry (b). Here we have assumed resources grow logistically with identical parameters as for semi-chemostat growth ($r = \delta = 0.1$, $K = R_{max} = 1$), as opposed semi-chemostat resource growth (main text). At the onset of the grey region, a supercritical Hopf-birfurcation emerges, after which stable limit cycles (not shown) surround unstable equilibria (thin red lines).

EMPIRICAL ANALYSIS OF METABOLIC SCALING WITH MASS AND TEMPERATURE

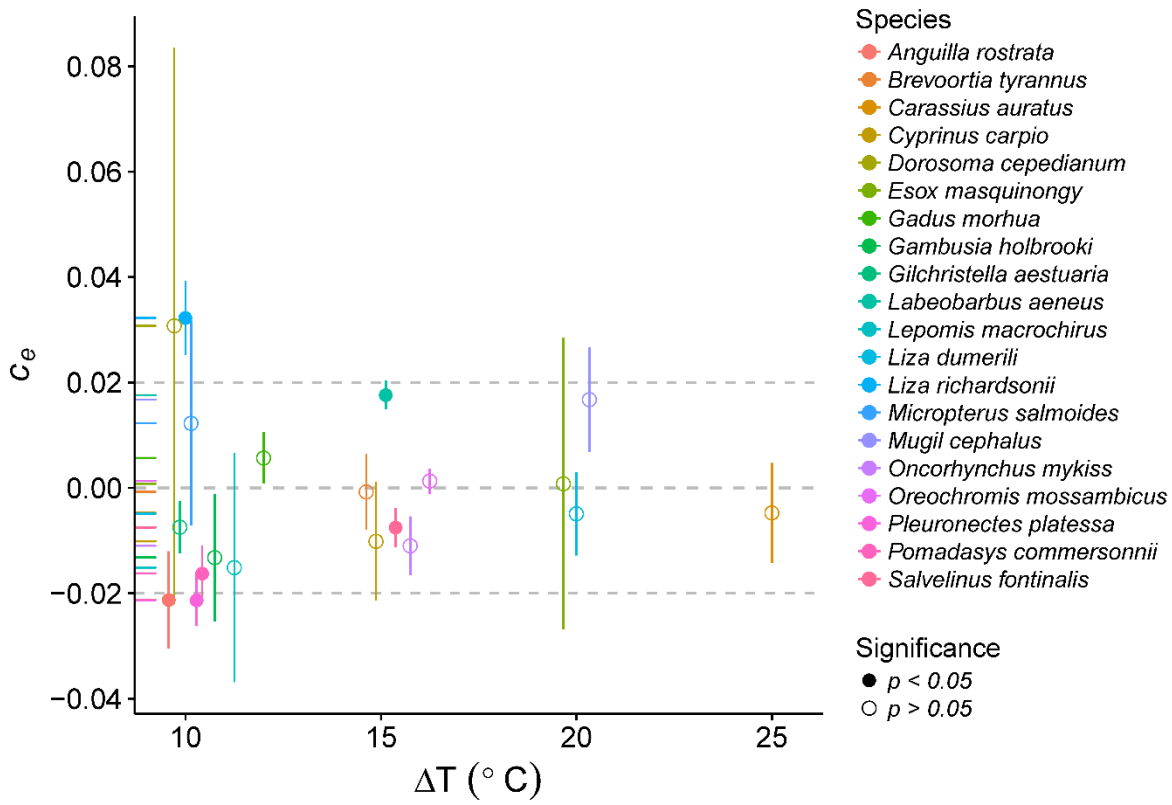

Figure S9 Results from estimation of the interaction between mass and temperature for the scaling of metabolic rate in 20 teleost fish species from experimental data. Estimates of the interaction coefficient, c_e, governing the temperature-dependence of the metabolic exponent within species (one estimate per species, n=20), plotted against the temperature range used for estimation. Vertical lines correspond to +/- one standard error. Points are color-coded by species. Closed circles correspond to significant interaction terms at the 0.05 significance level (n=6 species) and open circles indicate non-significant interactions (n=14 species). Dashed horizontal lines indicate a c_e-value of zero and the maximum and minimum values of the parameter c in the dynamic models.

Table S2 Table of effect sizes of the interaction-coefficient (c_e), corresponding p-values and standard error from empirical analysis of metabolic scaling models (see Eq. 4 in the main text). Bold text indicates significant interactions terms.

c_e	Temperature replicates	Species	ΔT	p	$s.e$	Mass range (g)
-0.0212	3	*Anguilla rostrata*	10	**0.0439**	0.0092	3.6-10400
-0.0007	4	*Brevoortia tyrannus*	15	0.9205	0.0072	5.4-80.9
-0.0047	9	*Carassius auratus*	25	0.6196	0.0095	178-1.6
-0.0101	7	*Cyprinus carpio*	15	0.3732	0.0113	4.4-3487
0.0307	7	*Dorosoma cepedianum*	10	0.5658	0.0528	3.9-256.9
0.0008	3	*Esox masquinongy*	20	0.9774	0.0276	9.6-19.2
0.0057	4	*Gadus morhua*	12	0.2466	0.0049	14.7-7100
-0.0132	3	*Gambusia holbrooki*	11	0.2993	0.0121	0.1-1.5
-0.0074	3	*Gilchristella aestuaria*	10	0.1524	0.0049	0.05-1.44
0.0176	4	*Labeobarbus aeneus*	15	**<0.0001**	0.0027	7.4-325.5
-0.0151	4	*Lepomis macrochirus*	11	0.4922	0.0218	5-133.5
-0.0049	5	*Liza dumerili*	20	0.5404	0.0079	4.41-79.6
0.0322	3	*Liza richardsonii*	10	**0.0005**	0.0071	2-54.9
0.0123	3	*Micropterus salmoides*	10	0.5417	0.0194	9-350
0.0168	5	*Mugil cephalus*	20	0.1010	0.0099	7.7-225
-0.0110	10	*Oncorhynchus mykiss*	16	0.0531	0.0056	4.2-1200
0.0013	5	*Oreochromis mossambicus*	16	0.5783	0.0024	10-150
-0.0213	3	*Pleuronectes platessa*	10	**0.0001**	0.0048	1-632
-0.0162	3	*Pomadasys commersonnii*	10	**0.0053**	0.0053	62.4-2627
-0.0075	4	*Salvelinus fontinalis*	15	**0.0448**	0.0037	5-1760

REFERENCES

Englund, G., Ohlund, G., Hein, C. L. & Diehl, S. 2011. Temperature dependence of the functional response. *Ecol. Lett.,* 14**,** 914-21.

Jobling, M. 1997. Temperature and growth: modulation of growth rate via temperature change. In *Global Warming: Implications for Freshwater and Marine Fish* (ed. Wood, C. M. and McDonald, D. G.), pp 225-254. Cambridge: Cambridge University Press.

Ohlberger, J., Langangen, Ø., Edeline, E., Claessen, D., Winfield, I. J., Stenseth, N. C. & Vøllestad, A. 2011. Stage-specific biomass overcompensation by juveniles in response to increased adult mortality in a wild fish population. *Ecology,* 92**,** 2175-2182. Beier, U. 2016. *Habitat use in fish communities: size- and environment-dependent mechanisms affecting biotic interactions and population regulation.* Doctoral Thesis, Swedish University of Agricultural Sciences.

Brown, J. H., Gillooly, J. F., Allen, A. P., Savage, V. M. & West, G. B. 2004. Toward a metabolic theory of ecology. *Ecology,* 85**,** 1771-1789.

Byström, P. & García-Berthou 1999. Density dependent growth and size specific competitive interactions in young fish. *Oikos,* 86**,** 217-232.

de Roos, A. M. & Persson, L. 2013. *Population and community ecology of ontogenetic development*, Princeton University Press.

de Roos, A. M., Schellekens, T., van Kooten, T., van de Wolfshaar, K., Claessen, D. & Persson, L. 2007. Food-dependent growth leads to overcompensation in stage-specific biomass when mortality increases: the influence of maturation versus reproduction regulation. *Am. Nat.,* 170**,** E59-E76.

Englund, G., Öhlund, G., Hein, C. L. & Diehl, S. 2011. Temperature dependence of the functional response. *Ecol. Lett.,* 14**,** 914-21.

Froese, R., Thorson, J. T. & Reyes, R. 2014. A Bayesian approach for estimating length-weight relationships in fishes. *J. Appl. Ichthyol.,* 30**,** 78-85.

Gilbert, B., Tunney, T. D., McCann, K. S., DeLong, J. P., Vasseur, D. A., Savage, V., Shurin, J. B., Dell, A. I., Barton, B. T., Harley, C. D., Kharouba, H. M., Kratina, P., Blanchard, J. L., Clements, C., Winder, M., Greig, H. S. & O'Connor, M. I. 2014. A bioenergetic framework for the temperature dependence of trophic interactions. *Ecol. Lett.,* 17**,** 902-14.

Gillooly, J. F., Brown, J. H., West, G. B., Savage, V. M. & Charnov, E. L. 2001. Effects of size and temperature on metabolic rate. *Science***,** 2248-2251.

Hjelm, J. & Persson, L. 2001. Size-dependent attack rate and handling capacity: inter-cohort competition in a zooplanktivorous fish. *Oikos,* 95**,** 520-532.

Hölker, F. 2000. *Bioenergetik dominanter Fischarten (Abramis brama (Linnaeus, 1758) und Rutilus rutilus (Linnaeus, 1758)) in einem eutrophen See Schleswig-Holsteins: Ökophysiologie und individuen-basierte Modellierung.* Doctoral Thesis, Verein zur Förderung der Ökosystemforschung zu Kiel.

Hölker, F. & Haertel, S. S. 2004. Application of a bioenergetics model to roach. *J. Appl. Ichthyol.,* 20.

Jobling, M. 1997. Temperature and growth: modulation of growth rate via temperature change. In *Global Warming: Implications for Freshwater and Marine Fish* (ed. Wood, C. M. and McDonald, D. G.), pp 225-254. Cambridge: Cambridge University Press.

Karås, P. & Thoresson, G. 1992. An application of a bioenergetics model to Eurasian perch (*Perca fluviatilis* L.). *J. Fish Biol.,* 41**,** 217-230.

Lumb, C. E., Johnson, T. B., Cook, H. A. & Hoyle, J. A. 2007. Comparison of lake whitefish (Coregonus clupeaformis) growth, condition, and energy density between Lakes Erie and Ontario. *J. Great Lakes Res.,* 33**,** 314-325.

Mitchell, S. E., Halves, J. & Lampert, W. 2004. Coexistence of similar genotypes of Daphnia magna in intermittent populations: response to thermal stress. *Oikos,* 106**,** 469-478.

O'Connor, M. I., Gilbert, B. & Brown, C. J. 2011. Theoretical predictions for how temperature affects the dynamics of interacting herbivores and plants. *Am. Nat.,* 178**,** 626-38.

Ohlberger, J., Edeline, E., Vollestad, L. A., Stenseth, N. C. & Claessen, D. 2011a. Temperature-driven regime shifts in the dynamics of size-structured populations. *Am. Nat.,* 177**,** 211-23.

Ohlberger, J., Langangen, Ø., Edeline, E., Claessen, D., Winfield, I. J., Stenseth, N. C. & Vøllestad, A. 2011b. Stage-specific biomass overcompensation by juveniles in response to increased adult mortality in a wild fish population. *Ecology,* 92**,** 2175-2182.

Ohlberger, J., Mehner, T., Staaks, G. & Hölker, F. 2012. Intraspecific temperature dependence of the scaling of metabolic rate with body mass in fishes and its ecological implications. *Oikos,* 121**,** 245-251.

Pauly, D. 1980. On the interrelationships between natural mortality, growth parameters, and mean environmental temperature in 175 fish stocks. *Journal du Conseil,* 39**,** 175-192.

Persson, L. & de Roos, A. M. 2013. Symmetry breaking in ecological systems through different energy efficiencies of juveniles and adults. *Ecology,* 94**,** 1487-1498.

Peters, R. H. 1983. *The ecological implications of body size*, Cambridge University Press.

Pothoven, S. A., Nalepa, T. F., Madenjian, C. P., Rediske, R. R., Schneeberger, P. J. & He, J. X. 2006. Energy density of lake whitefish Coregonus clupeaformis in Lakes Huron and Michigan. *Environ. Biol. Fishes,* 76**,** 151-158.

Savage, V. M., Gillooly, J. F., Brown, J. H., West, G. B. & Charnov, E. L. 2004. Effects of body size and temperature on population growth. *Am. Nat.,* 163**,** 429-441.

Stoessel, D. J. 2014. Age, growth, condition and reproduction of roach Rutilus rutilus (Teleostei: Cyprinidae), in south-eastern Australia. *Mar. Freshwat. Res.,* 65**,** 275-281.

Uszko, W., Diehl, S., Englund, G. & Amarasekare, P. 2017. Effects of warming on predator-prey interactions: a resource-based approach and a theoretical synthesis. *Ecol. Lett.,* 20**,** 513-523.

van Leeuwen, A., de Roos, A. M. & Persson, L. 2008. How cod shapes its world. *J. Sea Res.,* 60**,** 89-104.

Vasseur, D. A. & McCann, K. S. 2005. A mechanistic approach for modelling temperature-dependent consumer-resource dynamics. *Am. Nat.,* 166**,** 184-198.